

Experimental demonstration of non-line-of-sight visible light communication with different reflecting materials using a GaN-based micro-LED and modified IEEE 802.11ac

Zhijian Lu,^{1,2} Pengfei Tian,^{2,a} Houqiang Fu,¹ Jossue Montes,¹ Xuanqi Huang,¹ Hong Chen,¹ Xiaodong Zhang,¹ Xiaoyan Liu,² Ran Liu,² Lirong Zheng,² Xiaolin Zhou,² Erdan Gu,³ Yi Liu,^{2,b} and Yuji Zhao^{1,c}

¹*School of Electrical, Computer and Energy Engineering, Arizona State University, Tempe, Arizona 85287, USA*

²*Institute for Electric Light Sources, School of Information Science and Technology, Fudan University, Engineering Research Center of Advanced Lighting Technology, Ministry of Education, Shanghai 200433, China*

³*Institute of Photonics, Department of Physics, University of Strathclyde, Glasgow G1 1XQ, United Kingdom*

(Received 18 July 2018; accepted 6 September 2018; published online 12 October 2018)

This paper gives an experimental demonstration of non-line-of-sight (NLOS) visible light communication (VLC) using a single 80 μm gallium nitride (GaN) based micro-light-emitting diode (micro-LED). This device shows a 3-dB electrical-to-optical modulation bandwidth of 92.7 MHz. IEEE 802.11ac modulation scheme with 80 MHz bandwidth, as an entry level of the fifth generation of Wi-Fi, was employed to use the micro-LED bandwidth efficiently. These practical techniques were successfully utilized to achieve a demonstration of line-of-sight (LOS) VLC at a speed of 433 Mbps and a bit error rate (BER) of 10^{-5} with a free space transmit distance 3.6 m. Besides this, we demonstrated directed NLOS VLC links based on mirror reflections with a data rate of 433 Mbps and a BER of 10^{-4} . For non-directed NLOS VLC using a print paper as the reflection material, 16 QAM, 195 Mbps data rate, and a BER of 10^{-5} were achieved. © 2018 Author(s). All article content, except where otherwise noted, is licensed under a Creative Commons Attribution (CC BY) license (<http://creativecommons.org/licenses/by/4.0/>). <https://doi.org/10.1063/1.5048942>

I. INTRODUCTION

Today's wireless network is undergoing a transformation driven by the proliferation of data. Explosive growth in data-driven applications is placing unprecedented demands on communication systems. The performance of current Wi-Fi technology, however, is fundamentally limited due to the radio frequency (RF) spectrum crisis and is no longer sufficient to support future big data communication. Most recently, visible light communication (VLC) has emerged as a promising technology to mitigate the looming RF spectrum crisis as well as support a faster and safer wireless network for future communications. Thus, the essential techniques, including the fabrication of fast LEDs and optimization of the modulation scheme, have been widely investigated.

However, the limited bandwidth is the key factor of an LED-based optical source in VLC. Commercial LEDs based on blue LEDs and yellow phosphor usually have a modulation bandwidth of several MHz. Using a blue filter can increase the bandwidth to 20 MHz.¹ In comparison, micro-LEDs based on gallium nitride (GaN) offer much smaller carrier lifetimes and lower capacitance, which increases the bandwidth from several MHz¹ to hundreds of MHz.² On-off keying (OOK),

^aEmail: pftian@fudan.edu.cn

^bEmail: ylius@fudan.edu.cn

^cEmail: yuji.zhao@asu.edu

pulse-amplitude modulation (PAM) and orthogonal frequency division multiplexing (OFDM) have been used to achieve high-speed data communication up to 10 Gbps for one micro-LED,³ demonstrating the significant advantages of micro-LEDs in the application of VLC.

Regarding the VLC standard, the IEEE 802.15.7 VLC task group has completed a physical (PHY) and media access control (MAC) standard for VLC as of December 2011, with maximum data communication rate of 96 Mbps.⁴ It fails to consider the latest technological developments in the field of optical wireless communications, specifically with the wider bandwidth of GaN-based micro-LED and the introduction of optical orthogonal frequency-division multiplexing (O-OFDM) modulation methods which have been optimized for high data rates, multiple-access and energy efficiency. IEEE 802.11ac, widely used in 5G Wi-Fi communication, is a wireless networking standard based on OFDM modulation methods in the 802.11 families providing wider bandwidth (up to 80 MHz), high-density modulation (up to 256-QAM), and a single link high-throughput of up to 433 Mbps.^{5,6} Its 80 MHz channel bandwidth and 400 ns guard interval provides a data rate of 433 Mbps with a 256 QAM modulation scheme. Being able to use an IEEE 802.11ac based communication system⁷ provides a pathway towards merging Wi-Fi and VLC links, which can accelerate the practical application of VLC. In the future, VLC will be merged into Wi-Fi system, which is regarded as an alternative solution to commercial wireless communication system.

Line-of-sight (LOS) VLC using a GaN micro-LED achieves speeds on the order of Gbps in previous research,^{8,9} but its indoor communication scenario is not realistic. Non-line-of-sight (NLOS) VLC is more realistic,^{10,11} but there is few experimental demonstration, especially for micro-LEDs due to its small emission area and low optical output power. In this research, a packaged GaN-based micro-LED with a pixel size of $80\ \mu\text{m} \times 80\ \mu\text{m}$ was employed with a frequency response up to 92.7 MHz. We improved optics at both transmitter and receiver and enlarged the free space transmit range to 3.6 m for LOS VLC. We analyzed NLOS of the proposed VLC system using a micro-LED based on four kinds of reflection material such as mirror, ceramic, print paper, and photo paper. It demonstrated a high-speed VLC link for multi-path free space transmission using the modified IEEE 802.11ac standard and achieving a data rate of up to 433 Mbps.

II. EXPERIMENTAL DETAILS

We employed a single GaN-based micro-LED with a pixel size of $80\ \mu\text{m} \times 80\ \mu\text{m}$, fabricated from a commercially available LED wafer grown on a c-plane sapphire substrate. The LED had a conventional p-i-n structure with an n-GaN layer, InGaN/GaN multiple quantum wells (MQWs), an AlGaIn electron blocking layer and a p-GaN layer. First, Ni/Au (10nm/25nm) layers were deposited on top of the p-GaN, after which dry etching was employed to etch the Ni/Au layer and the GaN layers to form the mesas. P-contacts were formed by thermal annealing in purified air at 500 °C. Then, SiO₂ was deposited by plasma-enhanced chemical vapor deposition as the passivation layer, and apertures on the mesas were further defined by HF-based wet etching. Finally, Ti/Au (50nm/200nm) were deposited as the p-pad and n-pad to address each pixel individually. The micro-LEDs were packaged on a self-designed PCB and only the light emission from the sapphire side was used for VLC. The peak emission wavelength of the $80\ \mu\text{m} \times 80\ \mu\text{m}$ micro-LED is approximately 440 nm at a driving current 40 mA. To measure the -3dB modulation bandwidth of the packaged micro-LED, a small signal modulation from an Agilent N5225 network analyzer was combined with direct current from a Yokogawa GS610 source to drive the micro-LED. The emitted light was detected by a 1.4 GHz photodetector, after which the frequency response was read from the network analyzer.

IEEE 802.11ac has been used in RF band for high-throughput Wi-Fi. Here, we introduced IEEE 802.11ac wireless networking standard to VLC and modified its carrier frequency to approximately 50 MHz, which fit the electrical-to-optical modulation bandwidth of the micro-LED as discussed above. Because the carrier frequency is 50 MHz as the central band, the used band covers from 10 MHz to 90 MHz, which is within the -3dB electrical-to-optical modulation bandwidth of micro-LEDs. Fig. 1 demonstrates the proposed LOS VLC link using a single GaN micro-LED and modified IEEE 802.11ac wireless communication standard. We reproduced IEEE 802.11ac-based VLC link

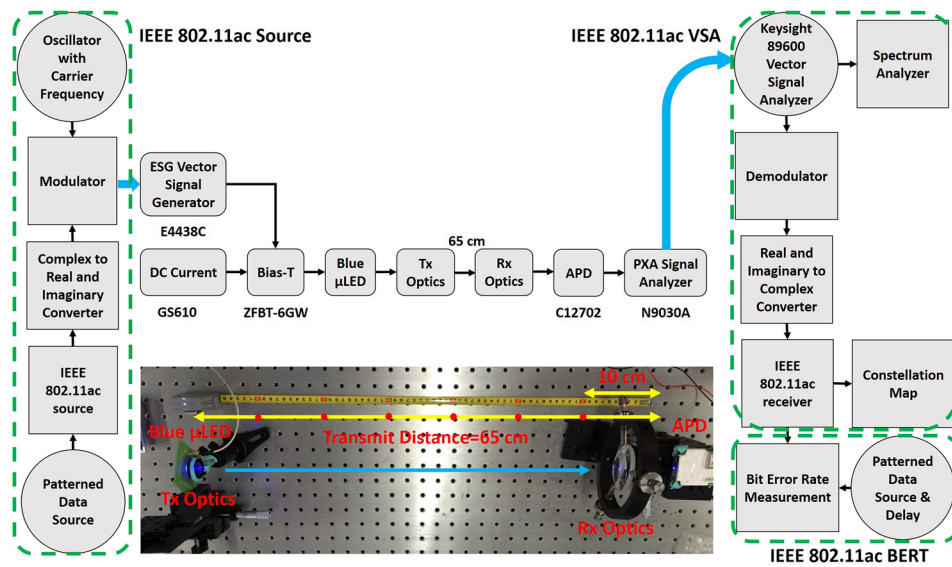


FIG. 1. LOS VLC using a GaN-based micro-LED and modified IEEE 802.11ac standard implementation by SystemVue including IEEE 802.11ac Source, IEEE 802.11ac VSA, and IEEE 802.11ac BER.

by SystemVue, which includes an IEEE 802.11ac source, an IEEE 802.11ac vector signal analyzer (VSA), and an IEEE 802.11ac bit error rate tester (BERT). The IEEE 802.11ac data source generated a PN15 data pattern. The IEEE 802.11ac source module generated IEEE 802.11ac-coded baseband signal with modulation coding scheme up to 256 QAM and a supported bandwidth of 80 MHz. The Complex to Real and Imaginary Converter model functioned as serial to parallel conversion at the transmitter. Digital data were converted into two-channel analog signals by digital-to-analog converters (DACs), which modulated IQ components of the optical carrier. The oscillator generated an RF (complex envelope) tone. Then M-ary quadrature amplitude modulation (M-QAM) baseband signal was modulated with the carrier frequency implemented by the modulator model, which then was downloaded to an ESG vector signal generator, Agilent E4438C. A DC bias, GS610, was added to the AC input signal by a Bias-T, Mini-Circuits ZFBT-6GW, driving the single GaN-based micro-LED. The light beam was concentrated by both transmitter and receiver optics in the 65 cm transmit distance and then captured by a high-sensitivity avalanche photodiode (APD), Hamamatsu C12702. The electrical output signal of the APD was detected by a PXA signal analyzer, Agilent N9030A. This IEEE 802.11ac receiver model was used to detect, demodulate and decode the baseband signal. In the IEEE 802.11ac VSA, it was captured by a Keysight 89600 vector signal analyzer. The Spectrum Analyzer model was used to measure the spectrum of a baseband signal. A coherent demodulator can be used to perform amplitude, phase, frequency, or I/Q demodulation. The Real and Imaginary to Complex Converter model converts real and imaginary input values to complex output values. After equalization, the output signal is ready for constellation of each spatial stream. In an IEEE 802.11ac BERT, the Delay model introduces a delay of N samples to the input signal, in this case a PN15 data pattern, to generate the reference. After the bit streams synchronization, the reference (REF) and test (TEST) inputs are compared for BER measurement.

In practical applications, the NLOS VLC link relies on the reflected light from the walls. For this scenario, we studied two commercially available reflection materials for directed NLOS: mirror and ceramic. As a control experiment, a mirror-based NLOS VLC setup with several reflections was established as shown in Fig. 2. The blue light is emitted from a GaN-based micro-LED and concentrated by a focus lens. Both the incident angle and reflected angle are 45° due to directed reflection. After a few reflections, the directed NLOS optical power is concentrated by the focus lens and captured by an APD. The size of the receiver antenna is 63 mm in diameter, and the focus length is 63 mm. The transmitter lens was specially designed for collimating the light

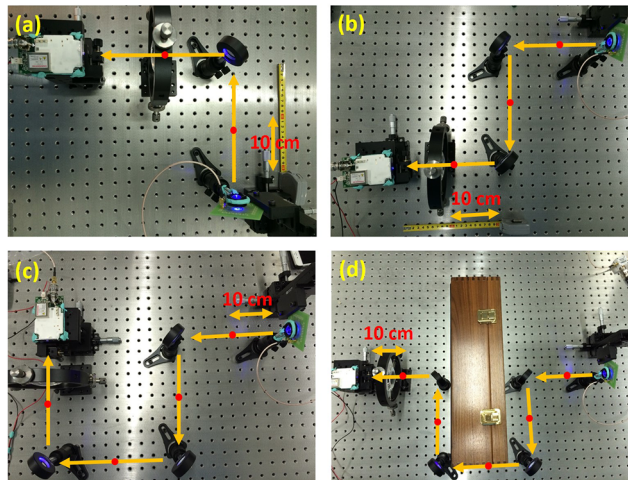


FIG. 2. (a) Mirror-based directed NLOS VLC setup with one reflection; (b) Mirror-based directed NLOS VLC setup with two reflections; (c) Mirror-based directed NLOS VLC setup with three reflections; (d) Mirror-based directed NLOS VLC setup with four reflections.

beam from the micro-LED. Through changing the distance between the transmitter (micro-LED) and the lens, the light beam divergence angle can be adjusted. The system performance is evaluated by the overall distance, the received power, the transmitted data rate with modulation mode, and BER.

With a non-directed NLOS link, the divergent beam of the communications between a transceiver and a large field-of-view (FOV) of the receiver depend on light reflections on the wall surfaces in the room. Two commercially available materials were used: print paper and photo paper. In comparison to the directed NLOS VLC setup, we added two optical lenses at the receiver in the non-directed NLOS VLC system as shown in Fig. 3(a) with careful alignment to focus the transmission beam and narrow the receiver FOV, which can support a feasible VLC link. In Figs. 3(b), (c), and (d), we fixed the 45° incident angle, the 40-cm free-space transmit distance, and changed the reflected angle to 10° , 45° , and 70° . The overall performance is measured by the reflected angle, the received power, the transmitted data rate with modulation mode, and BER.

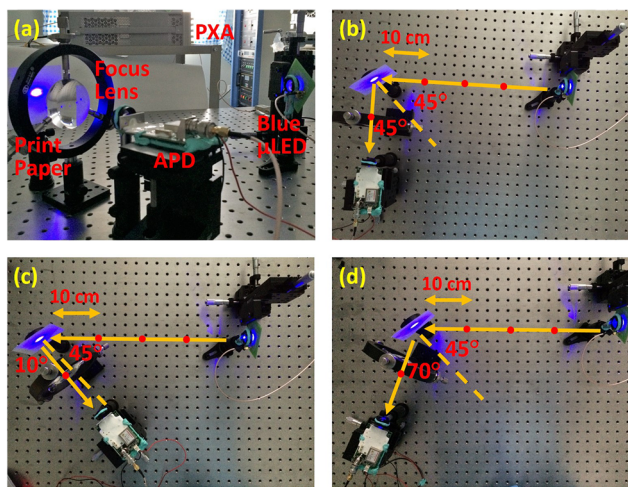


FIG. 3. (a) Print paper based non-directed NLOS VLC system; (b) Print paper diffuse reflection for 45° incident angle and 10° reflected angle; (c) Print paper diffuse reflection for 45° incident angle and 45° reflected angle; (d) Print paper diffuser reflection for 45° incident angle and 70° reflected angle.

III. RESULTS AND DISCUSSIONS

A. GaN-based micro-LED bandwidth

Fig. 4(a) shows that the electrical-to-optical modulation bandwidth of the micro-LED is 92.7 MHz at the 40 mA DC bias. Note that the micro-LED has a much higher bandwidth than 92.7 MHz, but packaging the micro-LEDs on a PCB limited the achieved bandwidth. However, the 92.7 MHz bandwidth is large enough for the 80 MHz IEEE 802.11ac standard. Improved packaging techniques, such as impedance matching, will be done in our future work. Fig. 4(b) shows the -3dB electrical-to-optical modulation bandwidth of the GaN-based micro-LED with DC bias from 10 mA to 100 mA. In this range, higher currents lead to the bandwidth increasing from 57.8 MHz to 107.6 MHz. Then the tendency keeps steady for the bandwidth saturation.

B. Optimal operating condition

The VLC link has been built by a single GaN-based micro-LED and modified IEEE 802.11ac standard, in which DC bias dominates the bandwidth of the micro-LED and the optical carrier frequency determines the band used in the modified IEEE 802.11ac standard. In the micro-LED bandwidth experiment, it shows that the bandwidth increases dramatically when DC bias goes up to 40 mA. If DC bias continually increases, the bandwidth will increase slightly because it is saturated by both PCB impedance matching and the micro-LED itself. Considering the aging characteristics of the micro-LED,¹² we chose 40 mA for the optimal operating conditions because larger DC bias might reduce the lifetime of the micro-LED. Besides, the larger DC bias over 40 mA leads to the higher light intensity, which might be threat to eye health.

Also, optical carrier frequency is the key factor to the VLC link band when using a modified IEEE 802.11ac standard. As 80 MHz channels were employed in VLC, a low optical carrier frequency moved the used band close to DC. Therefore, the quality of VLC became worse, because DC noise was brought into VLC. On the contrary, when a high optical carrier frequency was used, the band moved beyond the -3dB bandwidth (92.7 MHz) of the packaged micro-LED when the DC bias was at 40 mA. Fig. 5(a) demonstrates the relationship between DC bias and BER of VLC link. Fig. 5(b) demonstrates the relationship between optical carrier frequency and BER of the VLC link using a modified IEEE 802.11ac with 256 QAM modulation scheme. The VLC link with 50 MHz carrier frequency and 40 mA DC bias offers a BER of 6.2×10^{-5} . These characteristics proved that the optimal operating current is 40 mA and optical carrier frequency is 50 MHz.

C. LOS VLC

The LOS VLC using a GaN-based micro-LED and modified IEEE 802.11ac standard was established as shown in Fig. 2. According to this modified standard, the LOS VLC link at optimal operating condition using 80 MHz channels and 400 ns guard interval achieves a data rate of 433.3 Mbps and

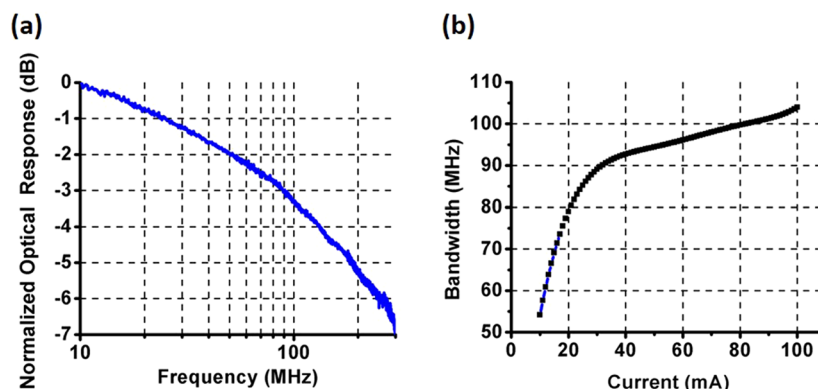


FIG. 4. (a) The frequency response of the packaged micro-LED under 40 mA DC bias. The extracted modulation bandwidth is 92.7 MHz. (b) The -3dB electrical-to-optical modulation bandwidth versus DC bias.

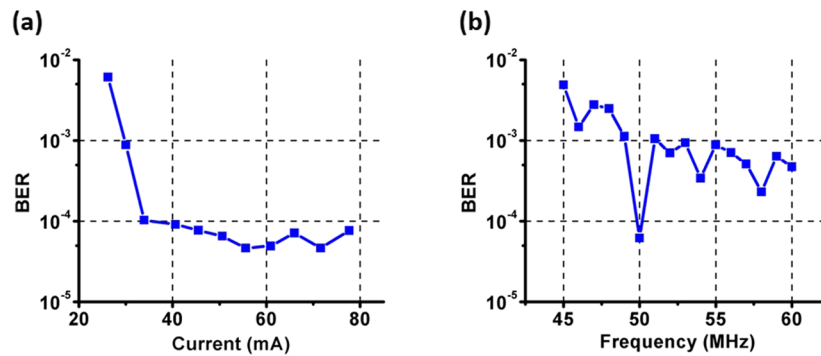


FIG. 5. (a) BER versus DC bias in VLC for 50 MHz optical carrier frequency and 256 QAM scheme. (b) BER versus optical carrier frequency in VLC at 40 mA DC bias with 256 QAM scheme.

a BER of 4.6×10^{-5} with a 256 QAM modulation scheme. Fig. 6(a) shows received power spectrum over a frequency range from 10 MHz to 90 MHz. The received power spectrum decreased by 6 dB approximately due to the -3dB bandwidth of the packaged micro-LED. Fig. 6(b) illustrates the received constellation maps for four modulation schemes including QPSK, 16 QAM, 64 QAM, and 256 QAM.

We also investigated the distance loss of LOS VLC within different distances over a range from 0.2 m to 3.6 m by measuring the received power and BER as shown in Fig. 7. The 3.6 m distance was limited by the size of our lab, and longer distance communication will be done in the future. It shows that received power decreased from 1.22 mW to 0.91 mW and thus BER kept a stable value of approximately 5×10^{-5} when the transmit distance increased. The distance loss largely depended on the proposed optics at both the transmitter and the receiver.

D. Directed NLOS VLC

Previous studies on VLC only assumed LOS between the transmitter and the receiver.^{8,9} Thus the transmission loss of indoor VLC is mainly related to the transmit distance, which determines the received optical power by LOS. In practice, the LOS light is usually blocked by obstacles between the transmitter and the receiver. Therefore, NLOS VLC link based on reflections can be utilized to keep communication functional.^{13,14} There are two kinds of transmission loss in NLOS VLC link: distance loss and reflection loss. The distance loss of LOS VLC link has already been discussed above. The mirror-based reflectivity is 0.91 while the ceramic-based reflectivity is 0.07 based on the

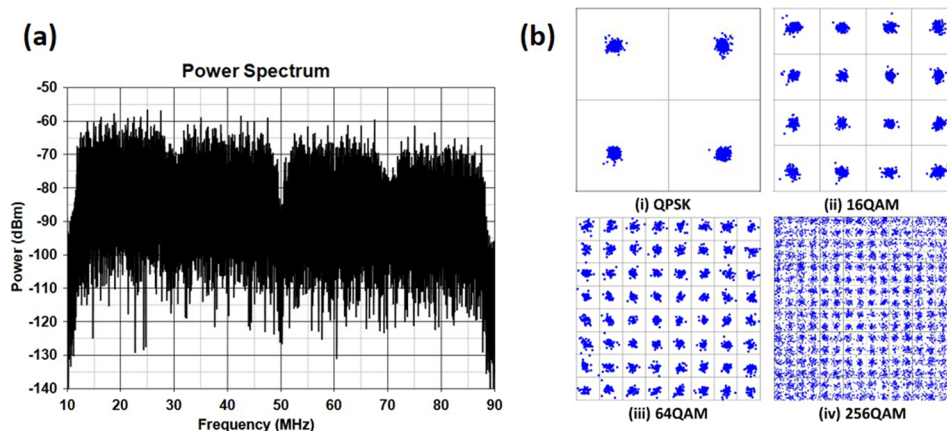


FIG. 6. (a) BER versus optical carrier frequency in VLC at 40 mA DC bias with 256 QAM scheme. (b) Received constellation maps of QPSK, 16 QAM, 64 QAM, and 256 QAM.

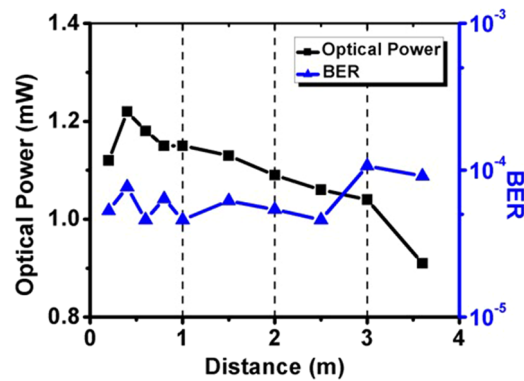


FIG. 7. Optical power and BER versus distance in LOS VLC using modified IEEE 802.11ac at 40 mA DC bias with 50 MHz optical carrier frequency.

incident optical power and reflected optical power. These results illustrate that the reflection loss is the principal loss in NLOS VLC.

Table I shows the system performance of directed NLOS VLC measured by the overall distance, the received power, transmitted data rate with modulation mode, and BER. The mirror-based NLOS VLC can still offer an effective high-speed communication link at a data rate of 433.3 Mbps and a BER of 10^{-5} . Ceramic, as the traditional wall material, was also employed in directed NLOS VLC. The result in Table I illustrates that after two ceramic-based directed reflections, the received optical power decreased dramatically to -22.22 dBm when background noise exerted a large impact to signal to noise ratio (SNR). Even if the SNR of the ceramic-based NLOS VLC cannot support the high-speed link with 256 QAM, the modified IEEE 802.11ac standard with QPSK modulation scheme can be applied to this link at a data rate of 97.5 Mbps and a BER of 9.3×10^{-5} . We can also conclude from this that the proposed VLC link is suitable for visible light communication with very weak light due to the combination of the high-sensitivity APD, noise resistive modulation scheme, large bandwidth of micro-LED, and proposed optics.

E. Non-directed NLOS VLC

Besides directed NLOS VLC, the non-directed NLOS VLC was demonstrated experimentally in our work. In the modeling literature,^{15,16} it has been found that the intensity via diffuse paths is much weaker than that via LOS paths. The power via an LOS path is about ten times higher than that via the first reflective path. In the non-directed NLOS VLC experiment in our work, the intensity via an LOS path is 37.3 times greater than that via the first print paper reflective path and 32 times higher than that via the first photo paper reflective path.

Table II shows the overall performance of non-directed NLOS VLC evaluated by the reflected angle, received power, transmitted data rate with modulation mode, and BER. Diffuse reflection of non-directed NLOS VLC was uniformly distributed in different reflection angles when using print paper. With a 45° incident angle light, non-directed NLOS VLC can provide an effective

TABLE I. Directed NLOS VLC using modified IEEE 802.11ac for 40 mA DC bias and 50 MHz Optical carrier frequency.

Direct Reflection Type	Overall Distance (cm)	Received Power (dBm)	Applied Modulation Mode	Data Rate (Mbps)	Data Rate (Mbps)
mirror reflection once	40	-0.27	256 QAM	433.3	1.27×10^{-4}
mirror reflection twice	60	-0.71	256 QAM	433.3	6.54×10^{-5}
mirror reflection three times	80	-3.47	256 QAM	433.3	5.54×10^{-5}
mirror reflection four times	100	-5.69	256 QAM	433.3	2.01×10^{-4}
ceramic reflection once	40	-12.22	64 QAM	325	5.15×10^{-5}
ceramic reflection twice	60	-22.22	QPSK	97.5	9.32×10^{-5}

TABLE II. Non-directed NLOS VLC using modified IEEE 802.11ac for 40 mA DC bias and 50 MHz Optical carrier frequency (reflection materials are print paper and photo paper).

Diffuse Reflection Type	Incident/Reflected Angle (degree)	Received Power (dBm)	Applied Modulation Mode	Data Rate (Mbps)	Data Rate (Mbps)
print paper reflection	45/10	-15.2	16 QAM	195	6.36×10^{-5}
print paper reflection	45/45	-15.2	16 QAM	195	6.36×10^{-5}
print paper reflection	45/70	-15.2	16 QAM	195	6.54×10^{-5}
photo paper reflection	45/15	-14.6	64 QAM	325	2.79×10^{-3}
photo paper reflection	45/45	-12.2	64 QAM	325	5.15×10^{-5}
photo paper reflection	45/75	-15.2	16 QAM	195	6.36×10^{-5}

communication link with 16 QAM modulation over the 40-cm free-space transmit distance at a data rate of 195 Mbps and a BER of 6.36×10^{-5} at different reflection angles. On the other hand, the photo paper-based demonstration shows a non-uniform distribution in diffuse reflection. With a 45° incident angle light, it can provide communication links with different modulation modes at different reflected angles. The photo paper experiment shows the characteristics of both the mirror-based directed reflection and the print paper-based diffuse reflection. When the reflected angle is 45° , using mirror-based reflection, it is possible to achieve 325 Mbps with 64 QAM modulation and a BER of 5.15×10^{-5} . When the angle is changed to 75° , the same BER can be achieved with 16 QAM modulation at a lower speed of 195 Mbps. However, when the reflected angle changes to 15° , keeping the 325 Mbps speed with 64 QAM modulation makes the quality of non-directed NLOS VLC decrease to a BER of 2.79×10^{-3} .

For validation,¹⁷ the bit error rate (P_b) is given by

$$P_b \approx \frac{4}{\log_2 M} Q\left(\sqrt{\frac{3\gamma_b \log_2 M}{M-1}}\right) \quad (1)$$

where the Q function is defined as:

$$Q(x) = \frac{1}{\sqrt{2\pi}} \int_x^\infty e^{-\frac{x^2}{2}} dx \quad (2)$$

Here, γ_b is defined as $\frac{E_b}{N_0}$, named SNR per bit. The measured results in Table I and Table II were validated by the theoretical calculations.

Furthermore, this work built the relationship between NLOS VLC performance and different kinds of reflection materials, which can offer constructive suggestions to the office wall decoration. The suitable office wall decoration can strengthen the reflective effect of NLOS VLC applications. In future NLOS VLC work, we expect that automatic alignment with mechanical system and integrated collimated lens will be achievable, to make this experiment further close to real world VLC applications.

IV. CONCLUSIONS

The NLOS VLC using a single GaN micro-LED was experimentally demonstrated in this work. For the feasibility of VLC, several advanced approaches were utilized such as the 92.7 MHz modulation bandwidth of the micro-LED, the modification of IEEE 802.11ac standard, and the proposed optics. All these techniques offered a high-speed LOS VLC at a data rate of 433 Mbps and a BER of 5×10^{-5} at a free space transmission distance of up to 3.6 m. Moreover, based on these techniques we also provided a possible VLC link in both directed NLOS and non-directed NLOS. Specially, non-directed NLOS VLC was achieved with 16 QAM modulation at a data rate of 195 Mbps and a BER of 10×10^{-5} via one reflection. Beyond theoretical analysis, the first experimental demonstration of practical implementation of NLOS VLC shows significance for indoor VLC system establishment.

ACKNOWLEDGMENTS

This work was supported in part by Bisgrove Scholar Program from Science Foundation Arizona, National Natural Science Foundation of China No. 61571135, and Fudan University Start-up Research Funding.

- ¹ P. Tian, J. J. McKendry, Z. Gong, S. Zhang, S. Watson, D. Zhu, I. M. Watson, E. Gu, A. E. Kelly, C. J. Humphreys, and M. D. Dawson, "Characteristics and applications of micro-pixelated GaN-based light emitting diodes on Si substrates," *J. Appl. Phys.* **115**(3), 1–6 (2014).
- ² M. Monavarian, A. Rashidi, A. Aragon, S. H. Oh, A. Rishinaramangalam, S. P. DenBaars, and D. Feezell, "Impact of crystal orientation on the modulation bandwidth of InGaN/GaN light-emitting diodes," *Appl. Phys. Lett.* **112**(4), 041104 (2018).
- ³ M. S. Islam, R. X. Ferreira, X. He, E. Xie, S. Videv, S. Viola, S. Watson, N. Bamiedakis, R. V. Penty, I. H. White, A. E. Kelly, E. Gu, H. Haas, and M. D. Dawson, "Towards 10 Gb/s orthogonal frequency division multiplexing-based visible light communication using a GaN violet micro-LED," *Photon. Res.* **5**, A35–A43 (2017).
- ⁴ R. Sridhar, R. D. Roberts, and S. Lim, "IEEE 802.15.7 visible light communication: Modulation schemes and dimming support," *IEEE Commun. Mag.* **50**(3), 72–82 (2012).
- ⁵ B. Sklar, *Digital communications* (Vol. 2) (Prentice Hall, 2001).
- ⁶ V. Kelly, "New IEEE 802.11 ac specification driven by evolving market need for higher, multi-user throughput in wireless LANs," IEEE Standards Association (2014).
- ⁷ E. Perahia and M. X. Gong, "Gigabit wireless LANs: An overview of IEEE 802.11 ac and 802.11 ad," *ACM SIGMOBILE Mobile Comput. Commun. Rev.* **15**(3), 23–33 (2011).
- ⁸ D. Tsonev, H. Chun, S. Rajbhandari, J. J. McKendry, S. Videv, E. Gu, M. Haji, S. Watson, A. E. Kelly, G. Faulkner, M. D. Dawson, H. Haas, and D. O'Brien, "A 3-Gb/s single-LED OFDM-based wireless VLC link using a gallium nitride μ LED," *IEEE Photon. Technol. Lett.* **26**(7), 637–640 (2014).
- ⁹ H. Chun, S. Rajbhandari, G. Faulkner, D. Tsonev, E. Xie, J. McKendry, E. Gu, M. Dawson, D. C. O'Brien, and H. Haas, "LED based wavelength division multiplexed 10 Gb/s visible light communications," *J. Lightw. Technol.* **34**(13), 3047–3052 (2016).
- ¹⁰ M. Saadi, L. Wattisuttikulkij, Y. Zhao, and P. Sangwongngam, "Visible light communication: Opportunities, challenges and channel models," *Int. J. Electron. Informat.* **2**(1), 1–11 (2013).
- ¹¹ W. Wang, C. Chow, L. Wei, Y. Liu, and C. Yeh, "Long distance non-line-of-sight (NLOS) visible light signal detection based on rolling-shutter-patterning of mobile-phone camera," *Opt. Express* **25**(9), 10103–10108 (2017).
- ¹² P. Tian, A. Althumali, E. Gu, I. M. Watson, M. D. Dawson, and R. Liu, "Aging characteristics of blue InGaN micro-light emitting diodes at an extremely high current density of 3.5 kA cm⁻²," *Semicond. Sci. Technol.* **31**(4), 045005 (2016).
- ¹³ D. Silage, *Digital Communication System Using System VUE* (Firewall Media, 2006).
- ¹⁴ A. K. Majumdar, "Non-line-of-sight (NLOS) ultraviolet and indoor free-space optical (FSO) communications," in *Advanced Free Space Optics (FSO)* (Springer, 2015).
- ¹⁵ G. Cossu, R. Corsini, and E. Ciaramella, "High-speed bi-directional optical wireless system in non-directed line-of-sight configuration," *J. Lightw. Technol.* **32**(10), 2035–2040 (2014).
- ¹⁶ M. S. Chowdhury, W. Zhang, and M. Kavehrad, "Combined deterministic and modified Monte Carlo method for calculating impulse responses of indoor optical wireless channels," *J. Lightw. Technol.* **32**(18), 3132–3148 (2014).
- ¹⁷ Y. Zhou, J. Shi, Z. Wang, J. Zhang, X. Huang, and N. Chi, "Maximization of visible light communication capacity employing quasi-linear pre-equalization with peak power limitation," *Mathematical Problems in Engineering* **2016**, 1–8.